Fizika Nizkikh Temperatur, 2011, v. 37, No. 1, p. 12–24

David Shoenberg and the beauty of quantum oscillations

V.M. Pudalov

P.N. Lebedev Physical Institute, 53 Leninskii prospekt, Moscow 117924, Russia
E-mail: pudalov@lebedev.ru

Received August 24, 2010

The quantum oscillation effect was discovered in Leiden, in 1930, by W.J. de Haas and P.M. van Alphen in magnetization measurement, and by L.W. Shubnikov and de Haas — in magnetoresistance. Studying single crystals of bismuth, they observed oscillatory variations of magnetization and magnetoresistance with magnetic field. Shoenberg, whose first research in Cambridge had been on bismuth, found that much stronger oscillations are observed when a bismuth sample is cooled to liquid helium rather than to liquid hydrogen, which had been used by de Haas. In 1938 Shoenberg came from Cambridge to Moscow to study these oscillations at Kapitza Institute where liquid helium was available at that time. In 1947, J. Marcus observed similar oscillations in zinc, that persuaded Shoenderg to return to this research, and, since then, the dHvA effect had been one of his main research topic. In particular, he developed techniques for quantitative measurements of the effect in many metals. Theoretical explanation of quantum oscillations was given by L. Onsager in 1952, and the analytical quantitative theory by I.M. Lifshitz and A.M. Kosevich in 1955. These theoretical advancements seemed to provide a comprehensive description of the effect. Since then, quantum oscillations were commonly considered as a tool for measuring Fermi surface extremal cross-sections and all-angle electron scattering times. However, in his pioneering experiments in 1960s, Shoenberg revealed the richness and deep essence of the quantum oscillation effect and showed how the beauty of the effect is disclosed under nonlinear conditions imposed by interactions in the system under study. It was quite unexpected, that under «magnetic interaction» conditions, the apparently weak effect of quantum oscillations may lead to such strong consequences as breaking the sample into magnetic (now called «Shoenberg») domains and the formation of an inhomogeneous magnetic state. Owing to his contribution to the field of quantum oscillations and superconductivity, Shoenberg is no doubt one of the 20th century's foremost experts. We describe the experiments on finding the quantitative parameters of electron–electron interaction, which are in line with the Shoenberg ideas that the quantum oscillations are modified by interactions and, hence, their analysis enables one to extract the quasiparticle interaction parameters.

PACS: **71.30.+h** Metal–insulator transitions and other electronic transitions;
72.15.Rn Localization effects (Anderson or weak localization);
73.40.Qv Metal–insulator-semiconductor structures (including semiconductor-to-insulator).

Keywords: quantum oscillations, two-dimensional carrier system, electron–electron interaction.

1. Introduction: correspondence with David Shoenberg

It is a privilege to be invited to contribute to this volume in honour of Professor David Shoenberg with whom I had an opportunity to communicate and whose papers I studied thoroughly in the past. In the early 1970s, I was a graduate student at the famous Institute for Physical Problems in Moscow, which is now named after P.L. Kapitza. Though I have never met David Shoenberg personally, of course, I knew much about his work with Kapitza in Cambridge and in Moscow and about his visits to Kapitza Institute in 1960s. A few years earlier, in 1966, my scientific supervisor, the outstanding experimentalist and Teacher, M.S. Khaikin, suggested me to develop a supersensitive dilatometer, as a topic for gradate project. The dilatometer, i.e. a device for measuring small displacements, was intended for measuring changes in the sample size in magnetic field. The microwave technique was the favorite subject in the Khaikin laboratory, and, not surprisingly, the dilatometer was a sort of a microwave cavity with a thin copper membrane and a needle-type coaxial conductor, which concentrated microwave energy near the region of the membrane deformation.

When my dilatometer started working reliably, it appeared that I could easily observe the nice phenomenon of quantum oscillations of size of the metallic single crystals placed in varying magnetic field at low temperatures. The oscillatory magnetostriction had, of course, the same origin as the de Haas–van Alphen (dHvA) effect, and from its amplitude I anticipated to extract information on electron coupling to the lattice potential, that is the so-called deformation potential. I was encouraged with this observation and ignored a common wisdom that says «avoid quantitative amplitude measurements when possible». Quite soon I realized that the measurements of the magnetostriction amplitude alone is insufficient to get quantitative information. In order to extract components of the deformation potential tenzor, one has also to measure the amplitude of the oscillatory magnetic moment, i.e., the dHvA effect.

Experimentalists know perfectly that absolute amplitude measurements for a single effect is a hard task, and amplitude measurements for two effects are still much harder. In those times, David Shoenberg carried out nice absolute measurements [1,2] of the dHvA effect amplitude, and each of his papers represented a piece of experimental art and deserved careful reading. However, the technique he used was incompatible with my microwave cavity dilatometer. Clearly, measurements of the two effects should be performed *in situ* during a single cooldown, because the oscillation amplitude is determined not only by controllable variables (temperature, magnetic field), but also by the sample «quality» (more exactly, the Dingle temperature [3]), which may vary from one cooldown to another.

The solution to the problem was found heuristically: it unexpectedly came during the experiment and had a direct relation to David Shoenberg! The situation was as follows: in my measurements, for signal extraction from noise, I used not a conventional field modulation technique with a lock-in amplifier and a slow magnetic field sweep, but an alternative technique with a multichannel analyzer and fast multiple sweeps of magnetic field within several seconds [4]. The measuring system was based on the frequency modulation method, developed by M.S. Khaikin and represented a heterodyne microwave receiver. Variations of the crystal size were measured as changes in frequency of the microwave oscillator that had the cavity — displacement sensor — in the feedback loop. For convenience, in the Khaikin laboratory, the experimental data was not only recorded by electronics but was also available to experimentalists in visual and audio form. Correspondingly, the intermediate frequency signal transposed to the audio range was fed, besides a frequency detector, to an ordinary loudspeaker. Taking measurements of the oscillatory magnetostriction late in the evening, in the silent laboratory, I heard that, upon cooling the sample down to 0.3 K, the tone of the audio frequency signal began to vary abruptly with magnetic field in a saw-tooth manner, rather than harmonically (see Fig. 1).

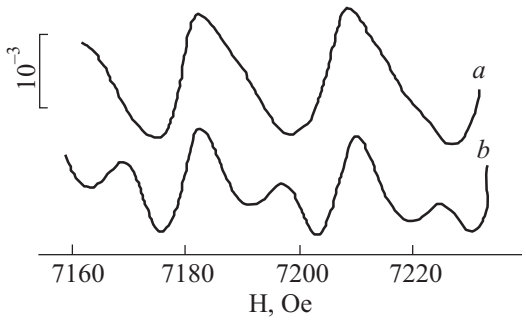

Fig. 1. Typical shape of the quantum oscillations of magnetostriction u_{11} of tin single crystal versus magnetic field. Bracket next to the upper curve depicts the magnetostriction scale. Temperature $T = 0.37$ K, $4\pi |dM/dH| \approx 0.18$: *a*) for $H \| [001]$ and *b*) for H tilted at 5° in the (010) plane. The lower curve reveals two groups of oscillations with frequency ratio $\approx 1:2$, due to two extremal cross-sections of the FS. Note a saw-tooth shape of oscillations. Reproduced from Ref. 6.

The first thought that in magnetic field the sample was cracking was rejected at once, because on subsequent warming of the sample up to 1.4 K, the oscillations became harmonic again, as expected. The observed unharmonicity was much greater, than one could expect from the Lifshitz–Kosevich (LK) theory [5]. Therefore, the more natural assumption was to associate the saw-tooth oscillations with the so-called Shoenberg effect and magnetic domains [2]. Indeed, despite the smallness of the magnetic moment oscillations δM, i.e., the amplitude of the dHvA effect, the oscillation period in good metals with a large Fermi surface (such as tin and indium under my investigation) is small and, therefore, the magnetic susceptibility $|\partial M / \partial B|$ becomes comparable with $1/4\pi$. As a result, the magnetic induction in the sample B noticeably deviates from the external magnetic field H :

$$B = H + 4\pi(1-D)M. \qquad (1)$$

The deviation leads to the magnetic interaction or the Shoenberg effect [2] (here D is the demagnetization factor), that is described by solution of the exact nonlinear equation [7]

$$M \sim \sum_{\nu} \sum_{r}^{\infty} A_{\upsilon}^{r} \sin\left[\left(\frac{\omega_c}{H + 4\pi(1-D)M}\right)\right]. \qquad (2)$$

As soon as the unharmonicity cause was identified, to make the next step was a matter of not too sophisticated though rather awkward calculations. Using sequential approximation technique I have calculated the discrete spectrum of oscillations. The obtained series converged rapidly and delivered a striking result: the desired amplitude of the magnetization oscillations could be found from the ratio of harmonics in the oscillatory magnetostriction spectrum. Therefore, the problem of simultaneous amplitude measurements for two effects reduced to measurements of the amplitude for only one of them supplemented with subsequent analysis of its spectrum.

This situation can be explained in the following way. Suppose we have a pendulum (oscillator) and wish to measure the amplitude of its oscillations, but there is no calibrated ruler to measure linear displacements. Then, for harmonic oscillator the problem has no solution. It appears, however, that for an unharmonic oscillator, when the physics of its unharmonicity is known, the oscillation amplitude may be found by registering the oscillation spectrum and analyzing the spectrum with a linear but uncalibrated ruler.

When the calculations of the oscillations spectrum were finished and successfully compared with experimental data, I was proud and assured with the result. It seemed convincing to me, and I was about to send the paper for publication. However, not all around me in the lab shared my assurance. The major expert in the field of quantum oscillations was certainly David Shoenberg and I decided to consult with him: I wrote a letter (e-mail didn't exist at that time) where I described my idea how the oscillation amplitude could be found from their spectrum under conditions of the magnetic interaction*. I was not sure that the famous scientist will answer to unknown graduate student. However, I was pleased to get a short note from Shoenberg quite quickly: he wrote that currently was busy but in a couple of weeks will be able to answer. I waited for about two weeks and indeed received a very kind letter: Shoenberg was positive about my idea, and also paid my attention to a potential «underwater stones», such as deviations from the conventional LK theory of oscillatory effects [5], which might be related, e.g., with mosaic structure of crystalline samples. These were the issues he studied at that time [8]. My paper was sent to the journal and published shortly [6]. I keep in memory the kind attention Shoenberg showed to an unknown graduate student, and try to educate my students in the same spirit of kindness and respect to others.

2. Interacting two-dimensional electron system

The experiments by Shoenberg demonstrated how the hidden beauty and rich essence of quantum oscillations are revealed in nonlinear conditions introduced by magnetic interaction. With another example of the beauty and richness of the quantum oscillations I faced much later, studying the electron–electron interaction effects in two-dimensional electronic system. This story is described below.

For pedagogical purposes, the story is delivered in the sequence as follows: firstly, we consider how the interparticle interaction modifies parameters of the electronic system, as compared with those for noninteracting gas. The interaction effects will be initially described, to a first approximation, in terms of the Fermi-liquid interaction constants. Further, we will consider the experimental method and the results of measurements of the Fermi-liquid interaction constants, where quantum oscillations are used as an experimental tool. We will presume first that the oscillation amplitude is small and is not strongly affected by interaction. And finally, we will consider how the interelectron interaction influences the quantum oscillation amplitude and what consequences it leads.

2.1. Renormalization of the quasiparticle parameters

As an Introduction, let us first recall that one of the major concepts for interacting Fermi systems is the Fermi liquid. It is the generalization of the Fermi gas, i.e. the system without interaction, to the case with interaction. The electrons in 3D metal or «metallic» 2D systems are charged and, at first sight, seem to experience a great Coulomb repulsion forces $\sim e^2/r_{ee}$, where r_{ee} is the interelectron distance; for 2D systems $r_{ee} \sim 1/\sqrt{n}$, where n is the electron density. In fact, these classical forces are compensated by ion lattice, because the total system is neutral. At low energies which matter most to us, additional (or trial) charges introduced to the system do not interact via the Coulomb potential. This is so, since the charges polarize their environment. In 3D, the long-range interaction has effectively been reduced to a short range one with a potential $\phi(r) \propto \exp(-r/r_{\rm sc})/r$ where $r_{\rm sc}$ is the screening length. The Fourier transform of the screening effect reads $1/q^2 \to 1/(q^2 + q_s^2)$, where q_s is the Thomas–Fermi wave vector which is inverse proportional to the screening length $r_{\rm sc}$.

In contrast to the 3D case, in 2D system the screening effect is much weaker. For large distance $rq_s \gg 1$, the asymptotic form of the average potential seen by the electrons [9] does not show an exponential decay

$$\bar{\phi}(r) \propto \frac{e}{q_s^2 r^3}. \qquad (3)$$

The essential idea on which Fermi-liquid theory is based was introduced by Landau. Even if the bare particles interact strongly, the low energy elementary excitations experience only a weak or moderate interaction. These elementary excitations are called quasiparticles. The quasiparticles can be labeled by the same quantum numbers as the excitations in the noninteracting system. In particular, in the vicinity of the Fermi surface they behave as if they were free fermions. In the absence of magnetic field the quasiparticles have the same charge and spin as free electrons, and for short, we shall call them «electrons». The interaction strength is characterized by the dimensionless ratio of the potential interaction energy E_{ee} to the kinetic (Fermi) energy, $r_s = E_{ee}/2E_F = me^2/\kappa\hbar^2\sqrt{\pi n} \propto 1/\sqrt{n}$ (here the factor of 2 takes the valley degeneracy in (100)-Si MOSFETs, $g_v = 2$, into account).

Within the framework of the Fermi-liquid theory, the interactions lead to renormalization of the effective quasiparticle parameters [10,11], such as the spin susceptibility

* This was the lucky time, when physicists shared with each other unpublished results, thoughts, and samples.

χ^*, effective mass m^*, Landé g-factor g^*, and compressibility κ^*. Measurements of these renormalized parameters are the main source of experimental information on interactions. The renormalization is commonly described by harmonics of the Fermi-liquid interaction in the singlet (symmetric, (s)) and triplet (antisymmetric, (a)) channels [10,12,13]:

$$\frac{g^*}{g_b} = \frac{1}{1+F_0^a}, \quad \frac{m^*}{m_b} = 1+\frac{1}{2}F_1^s,$$
$$\frac{\kappa^*}{\kappa_b} = \frac{m^*}{m_b}\frac{1}{1+F_0^s}, \quad \frac{\chi^*}{\chi_b} = \frac{m^*}{m_b}\frac{1}{1+F_0^a}. \qquad (4)$$

Here g_b, m_b, κ_b and χ_b are the band (bare) values of the g-factor, mass, compressibility and spin susceptibility, respectively. In theory, the above Fermi-liquid interaction constants $F_i^{a,s}$ are universal functions of the r_s solely. Provided the Fermi-liquid constants are known, the characteristics of the interacting 2D electron system to the first order can be expressed as interaction quantum corrections to the characteristics for the noninteracting 2D electron gas.

Though the results of numerical calculations of the renormalized parameters [14–17] vary considerably, all of them agree qualitatively and suggest enhancement of χ^*, m^* and g^* with r_s. Earlier experiments [18–21] have shown growth of m^* and g^*m^* at relatively small r_s values, pointing to a ferromagnetic type of interactions in the explored range $1 \lesssim r_s < 6.5$.

2.2. Quantum oscillations in the 2D electron gas as a tool for extracting interaction constants

For 3D noninteracting electron gas placed in quantizing magnetic field $H = H_z$, besides the quantized spectrum $\varepsilon_N = \hbar\omega_c(N+1/2)$ in the (k_x, k_y) plane there is a continuous spectrum along the magnetic field direction $\varepsilon(k_z)$. In contrast, for a 2D system of electrons placed in magnetic field $H_\perp$ perpendicular the (x,y) plane, the energy spectrum is fully quantized:

$$\varepsilon = \hbar\omega_c\left(N+\frac{1}{2}\right) \pm E_Z, \qquad (5)$$

where the Zeeman energy

$$E_Z = \frac{1}{2}g\mu_B H \qquad (6)$$

and $N = 0,1,2,...$ is the Landau level number. Each of the Landau levels is $\nu = H_\perp/\Phi_0$ times degenerate, and the oscillation period in the inverse magnetic field has a fundamental meaning being determined by the ratio of the electron density to the magnetic flux density, $n/(H_\perp/\Phi_0)$, where $\Phi_0 = hc/e$.

For noninteracting 2D electron gas, the theoretical expression for the Shubnikov–de Haas (SdH) effect, i.e. the oscillatory magnetoresistance, is as follows [5,22]:

$$\frac{\delta\rho_{xx}}{\rho_0} = \sum_s A_s \cos\left[\pi s\left(\frac{\hbar c\pi n}{eH_\perp}-1\right)\right]Z_s, \qquad (7)$$

where

$$A_s = 4\exp\left(-2\pi^2 s\frac{k_B T_D}{\hbar\omega_c}\right)\frac{2\pi^2 s k_B T/\hbar\omega_c}{\sinh(2\pi^2 s k_B T/\hbar\omega_c)}. \qquad (8)$$

Here $\rho_0 = \rho_{xx}(H_\perp = 0)$, $\omega_c = eH_\perp/(m^* m_e c)$ is the cyclotron frequency, m^* is the dimensionless effective mass, m_e is the free electron mass. This is the famous Lifshitz–Kosevich formula [5], modified for the 2D case [22]. An additional exponential factor describes Landau level broadening due to temperature-independent scattering by short-range impurity potential, $T_D \equiv \hbar/2\pi\tau_D$ is the so-called Dingle temperature [3], and τ_D is the «all angle» scattering time (in contrast to the transport time τ determined by large angle scattering).

In the limit of weak oscillations $\delta\rho_{xx}/\rho_0 \ll 1$ when temperature is not too low, Eq. (8) can be simplified:

$$A_s \approx 4\exp\left(-2\pi^2 s\frac{k_B(T_D+T)}{\hbar\omega_c^*}\right)4\pi^2 s\frac{k_B T}{\hbar\omega_c}. \qquad (9)$$

In Eqs. (7), (8) the valley splitting is assumed $g_v = 2$ (that corresponds to the 2D layer of electrons at the (100)-Si surface). The Zeeman factor in Eq. (7)

$$Z_s = \cos[\pi^2 s\hbar c(n_\uparrow - n_\downarrow)/(eH_\perp)] \qquad (10)$$

for $H_\parallel = 0$ reduces to a field-independent constant. Here $(n_\uparrow - n_\downarrow)$ is the difference in population of the two spin subbands. In case the spin magnetization is a linear function of the total field $H_{\rm tot}$, the nonzero difference in subbands populations, i.e. the spin polarization P, can be related to the renormalized spin susceptibility χ^* as follows:

$$P \equiv \frac{n_\uparrow - n_\downarrow}{n} = \frac{\chi^* H_{\rm tot}}{g_b\mu_B n} = g^* m^* \frac{eH_{\rm tot}}{nhc}, \qquad (11)$$

where $g_b \simeq 2$ is the bare g-factor for Si, and $H_{\rm tot} = \sqrt{H_\perp^2 + H_\parallel^2}$. Bychkov and Gorkov [23] have shown that the period of oscillations is not affected by interactions, whereas oscillation amplitude (Eqs. (9), (8)) is determined by $\omega_c^* = eH/(m^* m_e c)$ with the renormalized mass m^*, rather than the band mass m_b, and the Zeeman splitting (8) — by the renormalized g-factor.

2.3. The idea of measurements χ^*, m^*, and g^*

Experimental studies of magnetooscillations go back to the end of 60s when the high mobility 2D structures became available [20,24]. Information on the renormalized effective mass m^* is provided by the amplitude of the Shubnikov–de Haas (SdH) effect [23]. The effective mass is usually found from the so-called Dingle-plot,

$\ln(|\delta\rho_{xx}|/\rho_0)$ as a function of temperature. According to the LK theory, the damping factor can be expressed as

$$-\ln\left(A_1^{LK}\frac{\hbar\omega_c^*}{T}\right)\hbar\omega_c^* \approx (T+T_D)m^*. \qquad (12)$$

As follows from Eq. (12), in the limit of weak oscillations, $|\delta\rho_{xx}|/\rho_0 \ll 1$, the slope, $d\ln(|\delta\rho_{xx}|/\rho_0)/dT$, is nearly proportional to the effective mass m^*, whereas extrapolation of the $\ln[A_1(\hbar\omega_c/T)]$ to $T=0$ enables to determine T_D. Here, both, the effective mass and the *g*-factor are thermodynamic quantities and includes all many-body interaction effects.

The Zeeman factor Eq. (10) carries information on the renormalized spin susceptibility $\chi^* \propto m^* g^*$. Conventional technique to measure the effective χ^* [20,21] is based on the SdH measurements in magnetic fields tilted with respect to the 2D plane. In these measurements, the cyclotron energy related to $H_\perp$ is compared with the Zeeman splitting, which depends on the total field, $H_{\rm tot}$. To have a good control of both fields, the angle is to be measured with a very high accuracy, a difficult task at mK temperatures.

To probe separately orbital and spin degrees of freedom, it is convenient to apply two independently varied magnetic field components: (i) $H_\perp$, normal to the 2D electron plane, which causes quantization of the orbital motion, and (ii) the in-plane field $H_\parallel$, which couples only to spins. Application of $H_\parallel$ should facilitate the analysis of SdH oscillations, especially near the 2D metal–insulator transition, when the number of observable oscillations is small.

The idea of measurements with two field components is explained by Fig. 2. The parallel field $H_\parallel$ shifts the spin-up and spin-down subbands relative to each other in accord with Eqs. (5), (6), and produces an unequal population of the two subbands (see Eq. (11)). The role of the perpendicular field component is to provide measurements of the difference in subband population, and thus to extract the spin susceptibility according to Eq. (11). The perpendicular field causes quantization of the energy levels in both subbands and enables to count the difference in their individual population, because all spin-split Landau levels are exactly $H_\perp/(hc/e)$ times degenerate.

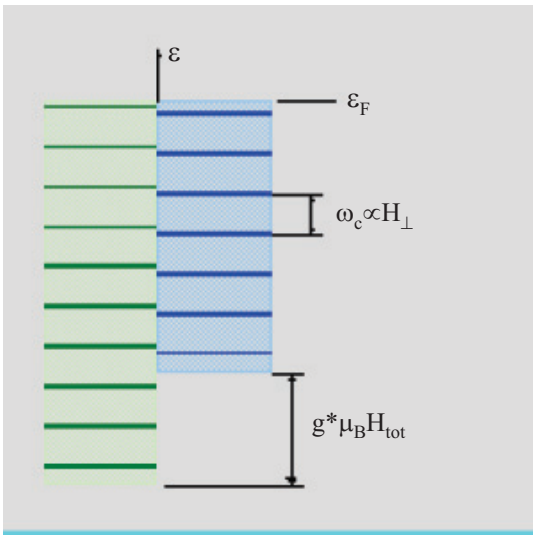

Fig. 2. Schematic diagram of the Landau levels in the presence of the Zeeman splitting $g^*\mu_B H_{\rm tot}$. The left and right ladders of Landau levels are for spin-up and spin-down subbands. $H_{\rm tot}=\sqrt{H_\perp^2+H_\parallel^2}$.

2.4. Crossed field technique

In order to facilitate measurements, we developed a «crossed-field technique» [25] by adding the second solenoid and taking data in crossed magnetic fields, which can be varied independently of each other (see Fig. 3). The conventional technique of measuring g^*m^* in tilted magnetic fields [20,21] is not applicable when the Zeeman energy is greater than half the cyclotron energy [26]. The crossed field technique removes this restriction and allows us to extend measurements over the wider range of electron densities. Development of this novel experimental technique enabled us to explore the effect of $H_\parallel$ on the electron spectrum, as well as to measure directly m^* and g^* in strongly correlated selectron systems [27].

Typical traces of the longitudinal resistivity ρ_{xx} as a function of $H_\perp$ are shown in Fig. 4. Due to the high elec-

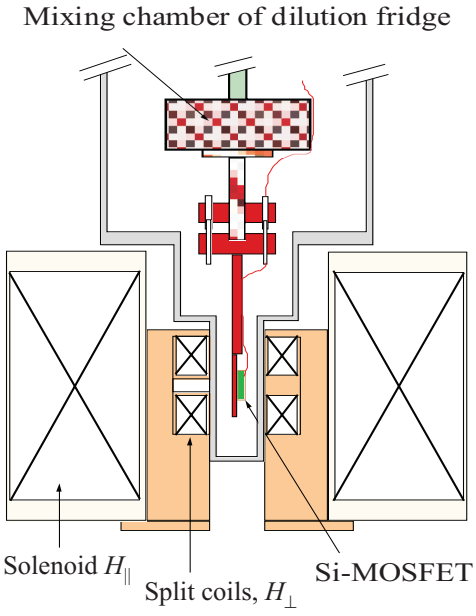

Fig. 3. The crossed magnetic field set-up. The main superconducting solenoid produces the in-plane magnetic field $H_\parallel$ up to 8 T. The superconducting split coils, positioned inside the main solenoid, produce the normal field $H_\perp$, which can be as large as 1.5 T at $H_\parallel \le 4$ T, and decreases gradually down to 0.6 T at $H_\parallel = 7.5$ T. The sample (Si-MOSFET) is attached to the cold finger of the mixing chamber, with its plane perpendicular to the axis of the coils. Represented from Ref. 25.

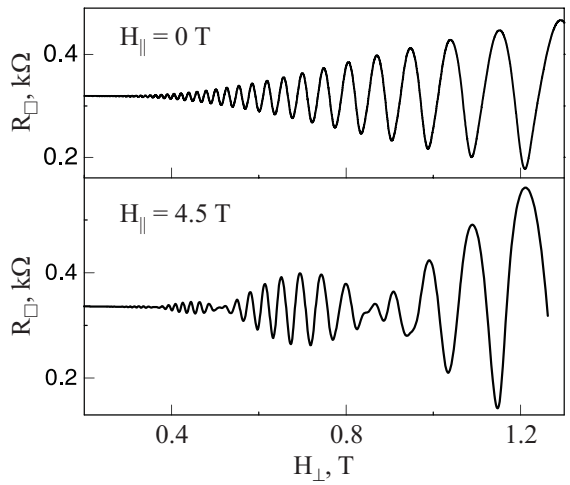

Fig. 4. Shubnikov–de Haas oscillations for $n = 10.6 \cdot 10^{11}$ cm^{-2} (Si-MOSFET sample) at $T = 0.35$ K [27].

tron mobility, oscillations were detectable down to 0.2 T and at temperatures up to 1.6 K; a large number of oscillations and wide range of temperatures enabled us to extract m^* and T_D with a high accuracy.

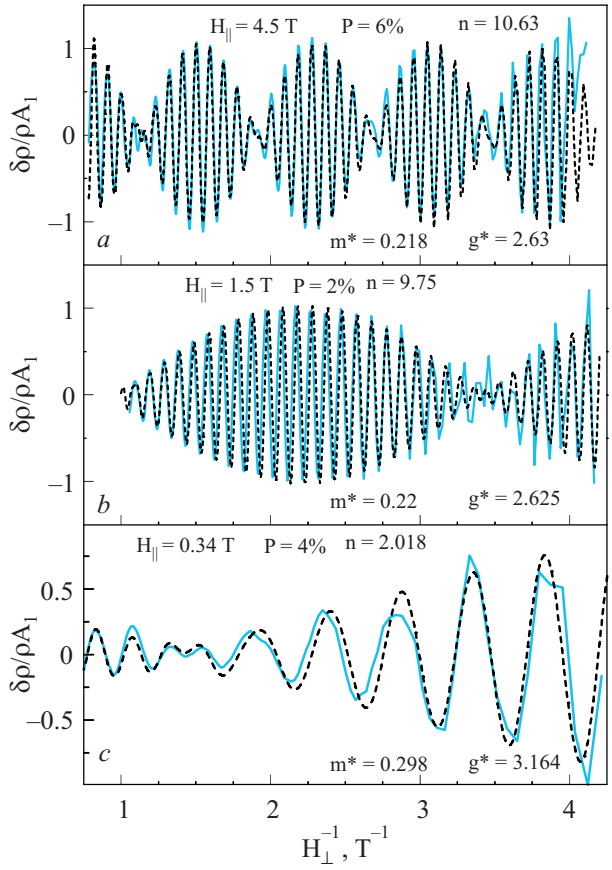

Fig. 5. Examples of fitting with Eq. (7): (*a*) $n = 10.6 \cdot 10^{11}$ cm^{-2}, $T = 0.35$ K, $H_{\|} = 4.5$ T, $P = 6$ % (the data corresponds to Fig. 1,*b*); (*b*) $n = 9.75 \cdot 10^{11}$ cm^{-2}, $H_{\|} = 1.5$ T, $P = 2$%; (*c*) $n = 2.02 \cdot 10^{11}$ cm^{-2}, $T = 0.2$ K, $H_{\|} = 0.34$ T, $P = 4$ %. The data are shown as the solid lines, the fits (with parameters shown) as dashed lines. All are normalized by $A_1(H_{\perp})$.

As Fig. 4 shows, application of $H_{\|}$ induces beating of SdH oscillations. This is because the uppermost levels in the two spin ubbands move with field at different rates and cross the Fermi energy either in phase or out of phase. The beatings are observed as a function of $H_{\perp}$ and the beat frequency is proportional to the spin polarization of the interacting 2D electron system P. In experiment, we observed a well pronounced beating pattern at a nonzero $H_{\|}$ (see Figs. 4 and 5), in agreement with Eq. (7). The phase of SdH oscillations remains the same between the adjacent beating nodes, and changes by π through the node. The interference pattern (including positions of the nodes) is controlled by Z_s in Eq. (7) and is defined solely by g^*m^*. Systematic study of this pattern enabled us to determine g^*m^* with high accuracy ($\sim 2\%$). The g^*m^* values are independent of T (at $T < 1$ K) within our accuracy [28]. We have observed a weak dependence of g^*m^* on $H_{\|}$ in strong $H_{\|}$. To determine g^*m^* in the linear regime, we systematically measured, for each n, the beating pattern at decreasing values of $H_{\|}$ until g^*m^* becomes independent of $H_{\|}$. Evolution of the beating pattern with $H_{\|}$ is illustrated in Figs. 5,*a* and *b*.

2.5. Data analysis

Comparison between the measured and calculated dependences $\delta\rho_{xx}/\rho_0$ versus $H_{\perp}$, both normalized by the amplitude of the first harmonic A_1 is shown in Fig. 5 for three carrier densities; for the sake of clarity, the oscillations are plotted as a function of the filling factor $\nu \propto 1/H_{\perp}$. The normalization assigns equal weights to all oscillations. We analyzed SdH oscillations over the low-field range $H_{\perp} \le 1$ T; this limitation arises from the assumption in Eq. (7) that $\hbar\omega_c \ll \varepsilon_F$ and $|\delta\rho_{xx}|/\rho_0 \ll 1$. The latter condition also allows us to neglect the inter-level interaction which is known to enhance g^* in stronger fields [29].

The amplitude of SdH oscillations at small $H_{\perp}$ can be significantly enhanced by applying $H_{\|}$ (see Fig. 6) [27], which is another advantage of the cross-field technique. Indeed, for low $H_{\perp}$ and n, the electron energy spectrum is complicated by crossing of levels corresponding to different spins/valleys. By applying $H_{\|}$, one can control the energy separation between the levels, and enhance the amplitude of low-field oscillations. We have verified that application of $H_{\|}$ (up to the spin polarization $\sim 20\%$) does not affect the extracted m^* values (within 10% accuracy), (the insets to Fig. 6 show that the values of m^* measured at $H_{\|} = 0$ and 3.36 T do coincide).

Fitting of the data provides us with two combinations of parameters: g^*m^* and $(T + T_D)m^*$. The first combination, $g^*m^*/2m_b$ normalized by the band values, represents the sought-for renormalized spin susceptibility. The measured values of g^*m^*, as well as m^* which are discussed below, were similar for different samples. Figure 7,*a* shows that for small r_s (high densities), our g^*m^* values agree with

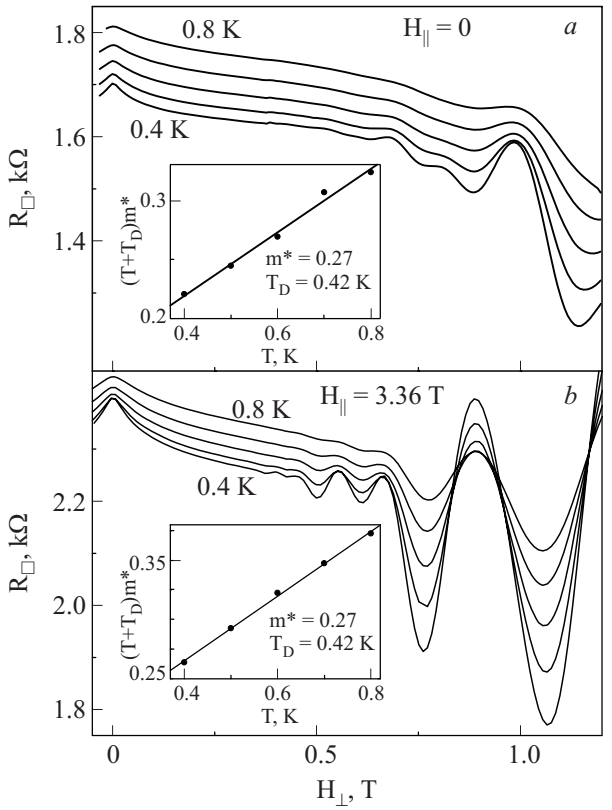

Fig. 6. Shubnikov–de Haas oscillations versus $H_\perp$ for $n = 2.2 \cdot 10^{11}$ cm^{-2} (i.e. $r_s = 5.6$) and $T = 0.4$; 0.5 ; 0.6 ; 0.7 ; 0.8 K: $H_\parallel = 0$ (*a*) and 3.36 T (*b*). The insets show the temperature dependences of fitting parameters $(T + T_D)m^*$.

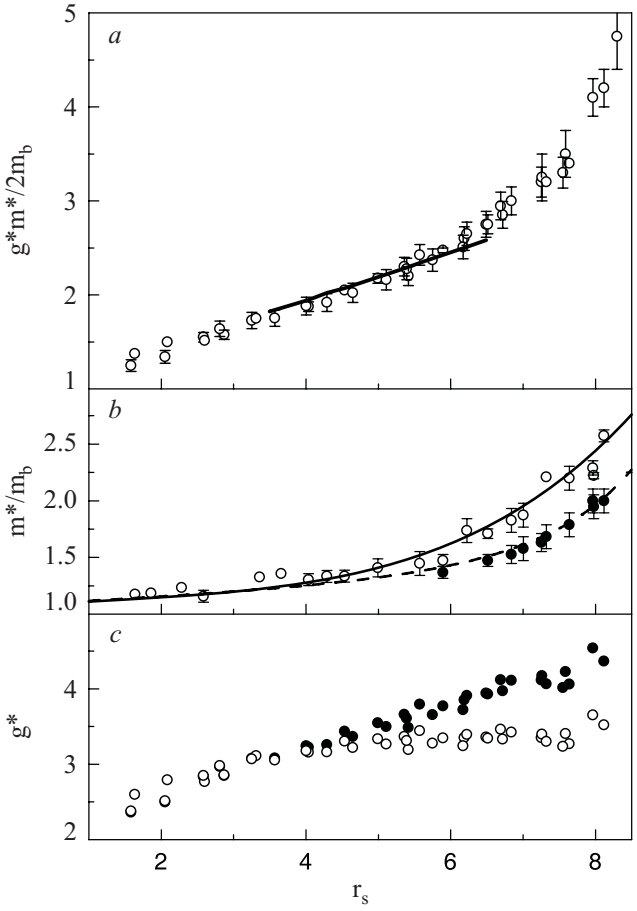

Fig. 7. Parameters g^*m^*, m^*, and g^* for different samples as a function of r_s (dots). The solid line in Fig. 7,*a* shows the data from Ref. 21. The solid and open dots in Figs. 7,*b* and 7,*c* correspond to two different methods of finding m^* (see the text). The solid and dashed lines in Fig. 7,*b* are polynomial fits for the two dependences $m^*(r_s)$. The values of g^* shown in Fig. 7,*c* were obtained by dividing the g^*m^* data by the smooth approximations of the experimental dependences $m^*(r_s)$ shown in Fig. 7,*b*.

the earlier data by Fang and Stiles [20] and Okamoto *et al.* [21]. For $r_s \geq 6$, g^*m^* increases with r_s faster than it might be expected from extrapolation of the earlier results [21].

The second combination, $(T + T_D)m^*$, controls the amplitude of oscillations. In order to disentangle T_D and m^*, we analyzed the temperature dependence of oscillations over the range $T = 0.3$–1.6 K (for some samples 0.4–0.8 K). The conventional procedure of calculating the effective mass for low r_s values ($\lesssim 5$), based on the assumption that T_D is T-independent, is illustrated by the insets in Fig. 6. In this small-r_s range, our results are in a good agreement with the earlier data by Smith and Stiles [19], and by Pan *et al.* [18]. The assumption of temperature independent T_D, however, becomes dubious at low densities (high r_s), where the resistance varies significantly over the studied temperature range; in this case, the two parameters T_D and m^* become progressively more correlated. The open dots in Fig. 7,*b* were obtained by assuming that T_D is T-independent over the whole explored range of n: m^* increases with r_s, and the ratio m^*/m_b becomes ~ 2.5 at $r_s = 8$ ($m_b = 0.19$ is the band mass). As another limiting case, one can attribute the change in $\rho(T)$ solely to the temperature dependence of the short-range scattering and request $T_D(\propto 1/\tau_D)$ to be proportional to $\rho(T)(\propto 1/\tau)$. In the latter case, the extracted dependence $m^*(r_s)$ is weaker (the solid dots in Fig. 7,*b*).

Our data shows that the combination $(T + T_D)m^*$ is almost the same for electrons in both spin-up and spin-down subbands (e.g., for $n = 3.76 \cdot 10^{11}$ cm^{-2} and $H_\parallel = 2.15$ T ($P = 20\%$), the T_D values for spin-up and spin-down levels differ by $\leq 3\%$). This is demonstrated by the observed almost 100% modulation of SdH oscillations (see, e.g., Figs. 5,*a* and 5,*b*). Thus, the carriers in the spin-up and spin-down subbands have nearly the same scattering time.

2.6. Comparison with other data

2.6.1. High density/weak interaction regime. As seen from Fig. 8, the data on *n*-channel Si-MOS samples are in a reasonable agreement with the data obtained by Zhu *et al.* [30] for *n*-type GaAs/AlGaAs samples from measurements of SdH effect in tilted magnetic field. Because of a smaller (by a factor of 3) electron effective mass in

GaAs, similar r_s values have been realized for the electron density 10 times lower than in Si-MOS samples. The width of the confining potential well in such GaAs/AlGaAs heterojunctions is greater by a factor of 6 than in (100) Si-MOS, due to a smaller mass m_z, lower electron density, and higher dielectric constant. This significant difference in the thickness of 2D layers may be one of the reasons for the 20% difference between the χ^*-data in *n*-GaAs and *n*-Si-MOS samples seen in Fig. 8; at the same time, the minor difference indicates that *the effect of the width of the potential well on renormalization of* χ^* *is not dramatic.*

The SdH experiments provide direct measurement of χ^* in weak perpendicular and in-plane magnetic fields $\hbar\omega_c \ll E_F$, $g^*\mu_B H_{\rm tot} \ll E_F$ [27]. Under such conditions, the quantum oscillations of the Fermi energy may be neglected, and, in the clean system, the magnetization should remain a linear function of H, $\chi^*(H_{\rm tot}) \approx \chi_0^*$. Also, under such experimental conditions, the filling factor is large, $\nu = nh/(eB_\perp) \gg 1$ and the amplitude of oscillations is small $|\delta\rho_{xx}|/\rho_{xx} \ll 1$. Figure 9 shows, on the $\rho - H_\perp$ plane, the domain of the weak magnetic fields, $\nu > 6$, where the SdH oscillations have been measured in Refs. 27, 31. As the perpendicular magnetic field increases further (and ν decreases), the SdH oscillations at high density $n \gg n_c$ transform into the quantum Hall effect; for low densities, $n \approx n_c$, the SdH oscillations transform into the so-called «reentrant QHE–insulator» (QHE–I) transitions [32]. The uppermost curve (open circles) presents the $\rho(H)$ variations in the regime of the QHE–I transitions [32], measured for a density slightly larger (by 4%) than the critical density value n_c for the metal–insulator transition. This diagram is only qualitative, because the n_c value is sample (disorder)-dependent.

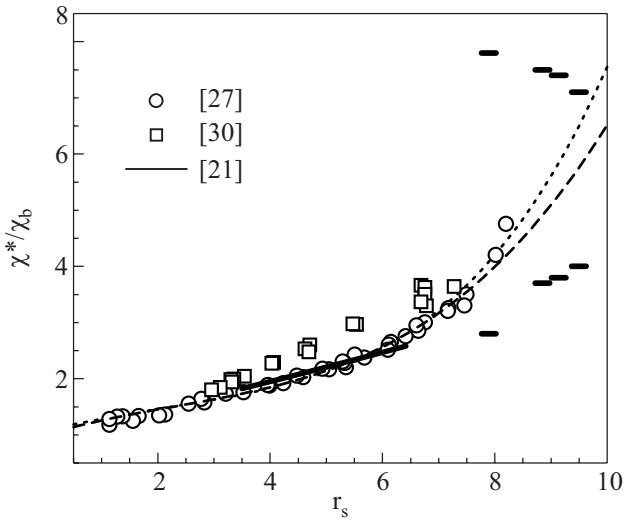

Fig. 8. Renormalized spin susceptibility measured by SdH effect in tilted or crossed fields on *n*-Si-MOS by Okamoto *et al*. [21], Pudalov *et al*. [27], and on *n*-GaAs/AlGaAs by Zhu *et al*. [30]. Horizontal bars depict the upper and lower limits on the χ^* values, determined from the sign of SdH oscillations, measured at $T = 0.027$ mK in Ref. 31. Dashed and dotted lines show two examples of extrapolation of the data [27].

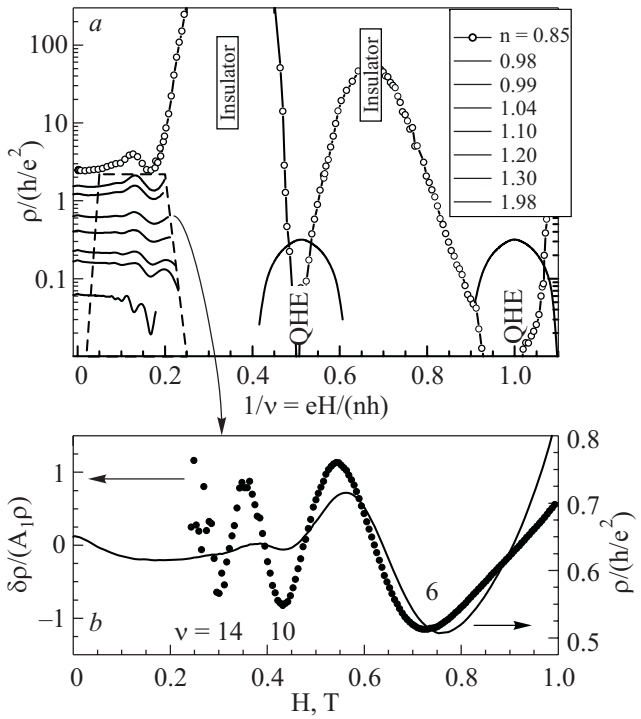

Fig. 9. (*a*) Overall view of the SdH oscillations in low fields at different densities. Empty circles show the ρ_{xx} oscillations for high-mobility Si-MOSFET sample in high fields, corresponding to the reentrant QHE–insulator transitions [32]. (*b*) Expanded view of one of the $\rho_{xx}(H)$ curves ($n = 1.04 \cdot 10^{11}$ cm^{-2} (right axis) and its oscillatory component normalized by $A_1(H)$ (left axis)) [27]. Dashed line confines the region of the SdH measurements in Refs. 27, 31.

2.6.2. Low density/strong interaction regime. In the vicinity of the critical density $n \approx n_c$, the number of observed oscillations decreases, their period increases, and the interpretation of the interference pattern becomes more difficult, thus limiting the range of direct measurements of $\chi^*(r_s)$.

The horizontal bars in Fig. 8 are obtained from consideration of the sign and period of SdH oscillations [31] as explained below. They show the upper limit for χ^*, calculated from the data reported in Refs. 27, 31, 32. Figure 9,*b* demonstrates that in the density range $0.7\ \text{cm}^{-2} < n < 1 \cdot 10^{11}\ \text{cm}^{-2}$, the oscillatory ρ_{xx} (beyond the magnetic field enhanced $\nu = 1$ valley gap) has minima at filling factors

$$\nu = (4i - 2), \qquad i = 1, 2, 3..., \tag{13}$$

rather than at $\nu = 4i$ (in (100) Si-MOSFETs, the valley degeneracy $g_\nu = 2$). The latter situation is typical for high densities and points to the inequality $g^*\mu_B B < \hbar\omega_c^*/2$.

In other words, the sign of oscillations at low densities is reversed. This fact is fully consistent with other observations (see, e.g., Fig. 2 of Ref. 31, Fig. 1 of Ref. 33, and

Figs. 1–3 of Ref. 34). As Fig. 8 shows, the ratio χ^*/χ_b exceeds $1/2m_b = 2.6$ at $r_s \approx 6$; the first harmonic of oscillations disappears at this density (so-called «spin-zero»), and the oscillations change sign for lower densities. The sign of the SdH oscillations is determined by the ratio of the Zeeman to cyclotron splitting [5,23]

$$\cos\left(\pi\frac{g^*\mu_B H}{\hbar\omega_c^*}\right) \equiv \cos\left(\pi\frac{\chi^*}{\chi_b}m_b\right), \qquad (14)$$

therefore, we concluded in Ref. 31 that, in order to have negative sign in the range $10 > r_s > 6$, the spin susceptibility χ^* must obey the following inequality:

$$2.6 = \frac{1}{2m_b} < \frac{\chi^*}{\chi_b} < \frac{3}{2m_b} = 7.9. \qquad (15)$$

Thus, Eqs. (13) and (15) enable us to set the upper and lower limits for χ^*, which are shown by horizontal bars in Fig. 8 at $r_s = 7.9$–9.5. As density decreases (and r_s increases), due to finite perpendicular fields, in which the SdH oscillations were measured, the condition of Eq. (15) becomes a bit more restrictive, which leads to narrowing the interval between the upper and lower bars [31].

3. Magnetooscillations in strongly interacting 2D electron system

In Sec. 2.2 above we used the semiclassical LK formula for noninteracting 3D case [5] and have made only transparent changes for the 2D electron spectrum [22]. We assumed that for the interacting system, the LK-formula remains applicable, when bare (band) quasiparticle parameters are replaced with their values renormalized by interaction. This assumption is examined in this section. We shall consider only the case of weak oscillations when they are exponentially damped by either disorder broadening of the Landau levels or temperature smearing of the Fermi energy. For simplicity, we call this the «low-magnetic field regime». In higher quantizing fields, deviations from the LK formula were found earlier [9,35,36] and attributed to the magnetic field dependent oscillatory renormalization of the effective *g*-factor and mass, due to the inter-Landau level interaction [37].

Magnetooscillations in the interacting 2D system were studied theoretically over the last 50 years. The main issue under investigation is whether the oscillations frequency, phase, and damping factor for the strong interaction case remain the same as in the noninteracting system Eq. (7) and whether the FL parameters in the LK formula can be taken at zero magnetic field. Bychkov and Gorkov [23] have found that the amplitude of oscillations Eq. (9), rather than their frequency, is renormalized by interaction. Fowler and Prange [38] and Engelsberg [39] showed that the electron–phonon scattering rate does not appear in the oscillations amplitude; Martin *et al*. [40] have shown that the inelastic electron–electron scattering does not contribute to the damping of magnetooscillations.

Recently, an important advancement has been made in theory [40,41] of magnetooscillations. It was shown that the LK formula, in general, is still applicable when the oscillations are exponentially small. However, due to the interference between electron–electron and electron–impurity interactions, damping factor in oscillations acquires an additional term in both the diffusive and ballistic regimes as follows [41]:

$$-\ln\left[A_1(T,H_\perp)\right]\frac{\hbar eH_\perp}{2\pi^2 m^* m_e c k_B} = (T+T_D) - \alpha(T), \qquad (16)$$

where

$$\alpha(T) = -T\frac{\delta m^*}{m^*} - T_D\left(\frac{\delta m^*}{m^*} - \frac{\delta\tau_D^*}{\tau_D^*}\right),$$

$$\frac{\delta m^*(T)}{m^*} = -\mathcal{A}\ln\left(\frac{E_F}{T}\right),$$

$$\frac{\delta\tau_D^*}{\tau_D^*} = \mathcal{A}\left[2\pi T\tau - \ln\left(\frac{E_F}{T}\right)\right],$$

$$\mathcal{A} = \left(1+\frac{15F_0^a}{1+F_0^a}\right)\frac{1}{4\pi^2\sigma_D}, \qquad (17)$$

and the factor 15 in the last line is the number of triplet terms for a system with two degenerate valleys.

Our numerical simulations show that within the relevant interval $T = 0.03$–0.8 K and $r_s \le 6$, the $\ln T$ terms in Eq. (17) can be replaced with a *T*-independent constant. By combining the LK result Eq. (7) with the interaction-induced corrections and replacing all $\ln T$ terms by a constant within our limited T range, we obtain the following linearized equation [42] in the ballistic regime for the short-range scattering (i.e. $\tau_D \approx \tau_{\rm tr}$):

$$-\ln\left[A_1(T,H_\perp)\right]\frac{\hbar eH_\perp}{2\pi^2 m^* m_e c k_B} = T + T_D(1+2\pi\mathcal{A}T\tau) =$$

$$= T + T_D\left(1-\frac{1}{2}\frac{\delta\sigma(T)}{\sigma_D}\right). \qquad (18)$$

This remarkable result means that the *T*-dependent correction to the Dingle temperature, $\delta T_D(T)/T_D$ is just one-half of the interaction correction to the conductivity [43] $\delta\sigma(T)/\sigma_D$. The factor 1/2 originates from the difference between the interaction corrections to the momentum relaxation time ($\delta\tau_{\rm tr}(T)$) and quantum scattering time [44] ($\delta\tau_D(T)$). We note that the empirical procedure used for finding m^* in our earlier paper (Ref. 27) was based on the assumption that $T_D^* = T_D\left[1-\delta\sigma(T)/\sigma_D\right]$, which differs from Eq. (18) by a factor of 1/2.

For the interacting case, Eq. (18), the linear *T*-dependence of $\ln A_1(T,H_\perp)$ holds to the first approximation. This is in agreement with our experiments [27] which

show that $\ln A_1(T, H_\perp)$ for high r_s varies linearly with temperature within the experimental range $T = 0.2$–1 K (see the inserts to Fig. 6).

3.1. Refinement of the extracted F_0^a values

At relatively high densities (which correspond to $r_s < 4$), the corrections to the LK result are insignificant within the studied T range. As r_s increases, the temperature dependences of the oscillation magnitude predicted by the LK theory Eq. (7) and the interaction theory Eq. (17) start deviating from each other. The values of $|F_0^a|$ extracted from SdH data using Eq. (18) *are smaller than those obtained with the LK theory* but larger than $|F_0^a|$ obtained with the empirical procedure used in Ref. 27. E.g., at $r_s = 6.2$, the F_0^a values obtained according to Eq. (18) and the empirical procedure of Ref. 27 are –0.40 and –0.45, respectively. In Ref. 42 we have reanalyzed the data of Ref. 27 using Eq. (18) and compared them with available results from other transport measurements.

The F_0^a values obtained in Ref. 42 from the analysis of SdH oscillations using the theories [5,41] (see Sec. 3) are plotted in Fig. 10. For comparison, we have also plotted the F_0^a values calculated in Ref. 42 from fitting the monotonic temperature and magnetic field dependences of the conductivity $\Delta\sigma(T)$ and $\Delta\sigma(H_\parallel)$ [42,45,46] with the theory [43]. There is a good agreement between all data.

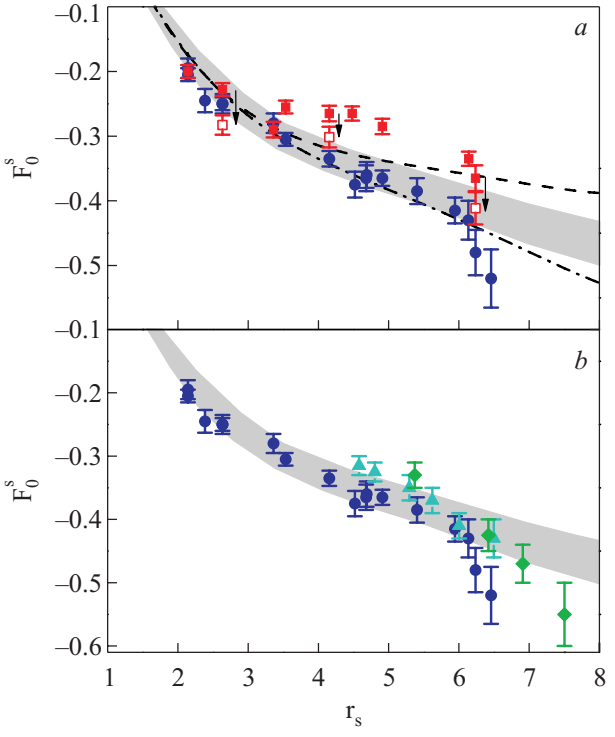

Fig. 10. (*a*) The dashed curve corresponds to $F_0^a(r_s)$ extracted from the SdH data [27] using the LK theory, the dash-dotted curve — to the empirical approach used in Ref. 27. The symbols depict F_0^a values obtained from fitting the transport data with the theory [43]. The shaded regions in panels (*a*) and (*b*) show the $F_0^a(r_s)$ dependence (with the experimental uncertainty) obtained from fitting our SdH data [27] with the theory [41]. (*b*) Comparison of F_0^a values recalculated from available $\delta\sigma(T, H = 0)$ data: dots — Ref. 42, triangles and diamonds — Refs. 45 and 46, respectively.

The spin susceptibility $\chi^* \propto g^* m^*$ obtained from SdH measurements appears to be almost T-independent [47], in apparent disagreement with the interaction correction theory [48] and renormalization group (RG) theory [49]. This contradiction could be resolved, provided the T-dependence of g^* is exactly compensated by the opposite T-dependence of m^*, so that $\chi^* \propto g^* m^*$ remains almost constant. The compensation, however, seems rather unlikely. We believe that the absence of temperature dependence in $g^* m^*$ values from SdH is simply a consequence of the cutoff that is imposed by finite magnetic fields $H_{\rm tot} > kT/g^*\mu_B$ which are applied in SdH measurements.

3.2. Other quasiparticle parameters extracted from SdH data

3.2.1. Valley splitting. The analysis of SdH oscillations using Eq. (7) also allowed us to estimate the value of the energy splitting [9] Δ_V between two valleys in the (100)-Si-MOSFET samples. A nonzero valley splitting causes beating of SdH oscillations. Figures 11,*a* and *b* show the SdH oscillations for two different samples. The electron densities are $6.1\cdot10^{11}$ and $1\cdot10^{12}$ cm^{-2}, respectively. The amplitude of weak SdH oscillations normalized by the first harmonic A_1 is expected to be field independent if $\Delta_V = 0$. A noticeable reduction in the SdH amplitude observed for both samples at small fields can be attributed to a finite valley splitting. Although the node of SdH oscillations expected at $H_\perp \approx 0.15$ T cannot be resolved for samples with mobilities ~ 2 m^2/(V·s), Δ_V can still be estimated from fitting of the $H_\perp$-dependence of the SdH amplitude with Eq. (7) modified for the case of a finite Δ_V: $\Delta_V = 0.4$ K for sample Si6-14 and 0.7 K for Si1-46. This estimate provides the upper limit for Δ_V at $H_\perp = 0$: in nonzero $H_\perp$ fields, Δ_V may be enhanced by the interlevel interaction effects [9,35,37].

3.2.2. Drude scattering time. The momentum relaxation time τ needed for calculating the interaction corrections was determined from the Drude conductivity $\sigma_D = ne^2\tau/m_b m_e$; the latter was found by extrapolating the quasi-linear $\sigma(T)$ dependence observed in the ballistic regime to $T = 0$ [43,50]. Note that in order to extract τ from the Drude conductivity, one should use the bare m_b rather than the renormalized effective mass: according to the Kohn theorem, the response of a translationally-invariant system to the electromagnetic field is described by m_b in the presence of electron–electron interactions; this result also holds for weak disorder ($E_F\tau \gg 1$). It is worth mentioning that several prior publications [45,46,50] incorrectly used m^* instead of m_b to estimate τ from σ_D; as

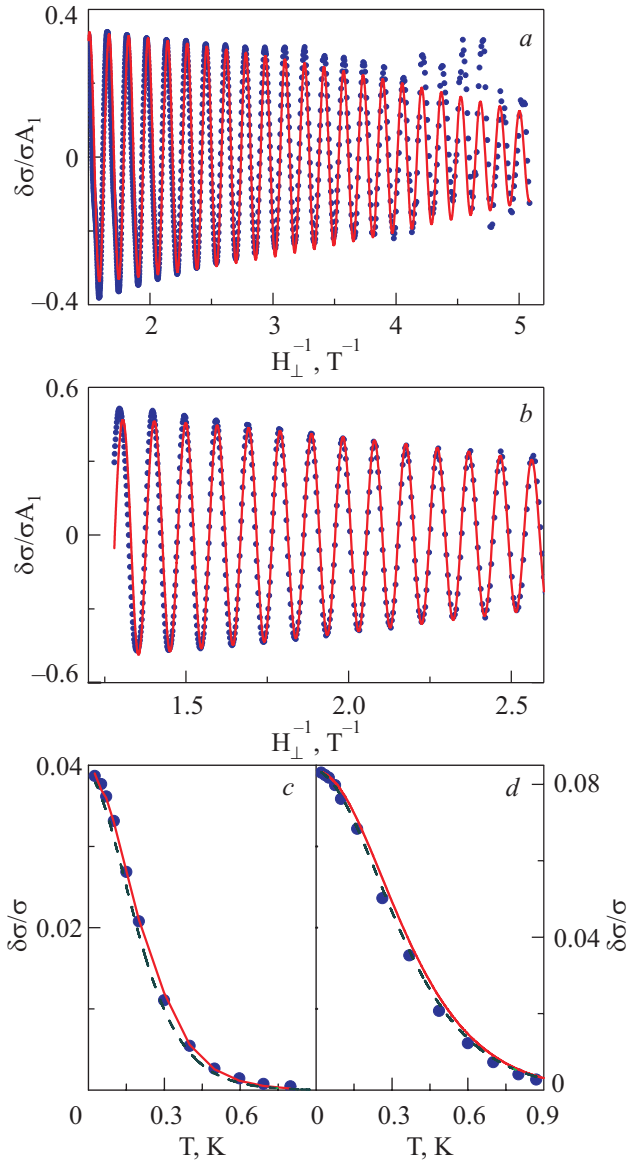

Fig. 11. SdH oscillations normalized by A_1: (*a*) sample Si6-14, n=6.1·10^{11}cm^{-2}, $T = 36$ mK; (*b*) sample Si1-46, n=1·10^{12} cm^{-2}, $T = 200$ mK. Dots show the data, solid curves — the theoretical dependences Eq. (7) modified for a finite $\Delta_V = 0.4$ and 0.7 K for samples Si6-14 and Si1-46, respectively. Panels (*c*) and (*d*) show the T-dependences of the SdH oscillations amplitude for Si6-14 ($n = 5.5\cdot10^{11}$ cm^{-2}) and Si1-46 ($n = 1\cdot10^{12}$ cm^{-2}), solid curves — the noninteracting LK-model Eq. (7), dashed curves — the fit based on the interaction theory Eqs. (17).

shown in Ref. 42, this affects the value of the fitting parameters extracted from comparison with the theory [43].

The textbook value [9] for the light electron mass in bulk Si is $m_b^{(3D)} \approx 0.19$. For inversion layers on (001) Si-surface [51], $m_b^{(2D)} = (0.19–0.22) \pm 0.02$ was found from tunneling measurements. The $m^*(n)$ data obtained from the analysis of SdH oscillations over a wide range of densities $r_s = 1.4–8.5$ [27], can be fitted with a polynomial $m^*(r_s) = 0.205(1 + 0.035r_s + 0.00025r_s^4)$. These m^* data agree well with earlier values of m^* extracted from SdH oscillations [19,20,24,52] in narrower ranges of densities. By extrapolating the polynomial $m^*(r_s)$ to $r_s = 0$ we obtain $m_b^{(2D)} = 0.205 \pm 0.005$; following Ref. 42 we adopted this value throughout the paper.

4. Conclusion

David Shoenberg was a great Master in experimental low-temperature physics. Besides the de Haas–van Alphen effect, he has made substantial contribution to understanding of the magnetic properties of superconductors. His book «Superconductivity» written in Moscow in 1938 is one of the reference books on my bookshelf and is used as a textbook by Russian students. Shoenberg's experiments on studying quantum oscillations in metals and the fine experimental techniques developed by him for this research represent a piece of experimental art. David Shoenberg has shown how the properties of interacting systems can be revealed by measuring quantum oscillations under nonlinear conditions imposed by interactions.

In line with this approach, we performed studies of the Shubnikov–de Haas effect for strongly interacting two-dimensional system of electrons. From the amplitude of quantum oscillations, we determined the interaction-induced renormalization of the quasiparticle parameters, such as the effective mass, spin susceptibility, and g-factor. The Fermi-liquid interaction parameter $F_0^a(n)$ obtained from the analysis of SdH oscillations agrees well with the $F_0^a(n)$ values obtained by fitting the monotonic transport data with the interaction correction theory [43]. However, it remains so far unclear how to reconcile the F_0^a values obtained at low electron densities from fitting the $\sigma(T)$ and SdH data (by using the interaction correction theory) with the corresponding values [53–55] obtained by fitting the $\sigma(T, H_{||})$ data with the RG theory. Possibly, for a quantitative description of the interaction effects in low temperature transport, the RG theory should be extended to a more realistic case of a finite intervalley scattering rate and to higher orders.

5. Acknowledgments

The author benefited from fruitful collaboration with M. Gershenson, H. Kojima, E.M. Dizhur, G. Bauer, G. Brunthaler, O.E. Omel'yanovskii, N.N. Klimov, D.A. Knyazev, A.Yu. Kuntsevich in performing measurements. The work was partially supported by grants from RFBR, Russian Academy of Sciences, and Russian Ministry for Education and Science (under contracts Nos. 02.552.11.7093, 14.740.11.0061, P2306, P798, P1234).

1. D. Shoenberg and J. Vanderkoy, *J. Low Temp. Phys.* **2**, 484 (1970).
2. D. Shoenberg, *Canad. J. Phys.* **46**, 1915 (1968); D. Shoenberg and I.M. Templeton, *ibid.* **46**, 1925 (1968).
3. R.B. Dingle, *Proc. Roy. Soc.* **A211**, 517 (1952).

4. V.M. Pudalov, *Dilatometric Studies of the Energy Spectrum of Conduction Electrons in Tin*, Chapter 7, in: Conduction Electrons, Moscow, Nauka (1985).
5. I.M. Lifshitz and A.M. Kosevich, *Zh. Eks. Teor. Fiz.* **29**, 730 (1955) [*Sov. Phys.-JETP* **2**, 636 (1956)].
6. V.M. Pudalov and M.S. Khaikin, *JETP* **40**, 1121 (1974) [*ZhETF* **67**, 2260 (1974)]; V.M. Pudalov, *Pis'ma ZhETF* 19(7), 466 (1974).
7. A.B. Pippard, *The Dynamics of Conduction Electrons*, Documents on Modern Physics (1965) [*Physica metallov. Electroni*, Moscow, Mir publisers (1972)].
8. D. Shoenberg, *J. Low Temp. Phys.* **25**, 755 (1976).
9. T. Ando, A.B. Fowler, and F. Stern, *Rev. Mod. Phys.* **54**, 437 (1982).
10. E.M. Lifshitz and L.P. Pitaevskii, *Statistical Physics*, Part II, Pergamon Press (1980).
11. A.A. Abrikosov, *Fundamentals of the Theory of Metals*, North-Holland, Amsterdam (1988).
12. A. Isihara, *Electron Liquids*, Springer-Verlag, Berlin (1997).
13. D. Pines and Nozier, *The Theory of Quantum Liquids*, W.A. Benjamin, Inc, NY (1966).
14. N. Iwamoto, *Phys. Rev.* **B43**, 2174 (1991).
15. Y. Kwon, D.M. Ceperley, and R.M. Martin, *Phys. Rev.* **B50**, 1684 (1994).
16. G.-H. Chen and M.E. Raikh, *Phys. Rev.* **B60**, 4826 (1999).
17. M. Marchi, S. De Palo, S. Moroni, and G. Senatore, *Phys. Rev.* **B80**, 035103 (2009).
18. W. Pan, D.C. Tsui, and B.L. Draper, *Phys. Rev.* **B59**, 10208 (1999).
19. J.L. Smith and P.J. Stiles, *Phys. Rev. Lett.* **29**, 102 (1972).
20. F.F. Fang and P.J. Stiles, *Phys. Rev.* **B174**, 823 (1968).
21. T. Okamoto, K. Hosoya, S. Kawaji, and A. Yagi, *Phys. Rev. Lett.* **82**, 3875 (1999).
22. A. Isihara and L. Smrčka, *J. Phys. C: Solid State Phys*. **19**, 6777 (1986).
23. Yu.A. Bychkov and L.P. Gor'kov, *Zh. Exp. Teor. Fiz.* **41**, 1592 (1961) [*Sov. Phys.-JETP* **14**, 1132 (1962)].
24. A.B. Fowler, F.F. Fang, W.E. Howard, and P.J. Stiles, *Phys. Rev. Lett.* **16**, 901 (1966).
25. M. Gershenson, V.M. Pudalov, H. Kojima, N. Butch, G. Bauer, G. Brunthaler, and A. Prinz, *Physica* **E12**, 585 (2002).
26. The common technique of measuring g^*m^* in tilted field is based on detecting the disappearance of the first harmonic of oscillations when $2g^*\mu_B H_{\rm tot} = \hbar eH_\perp / (m^*m_e)$. This technique is applicable only up to $r_s = 6.3$ [21].
27. V.M. Pudalov, M.E. Gershenson, H. Kojima, N. Butch, E.M. Dizhur, G. Brunthaler, A. Prinz, and G. Bauer, *Phys. Rev. Lett.* **88**, 196404 (2002).
28. Lacking of temperature dependence of the measured g^*m^* was apparently caused by a finite magnetic field which was always larger than temperature $H_{\rm tot} > kT / g^*\mu_B$ and therefore could cut-off the *T*-dependence if any.
29. The oscillatory behavior of the g^*-factor in strong $H_\perp$ is related to the exchange interaction between Landau levels. Particularly, this interaction leads to the enhancement of the g^*-value averaged over the period of oscillations (for the Si data, see V.M. Pudalov et al., *JETP* **62**, 1079 (1985)). For low magnetic fields and weak SdH effect regime, the inter-level interaction may be ignored.
30. J. Zhu, H.L. Stormer, L.N. Pfeiffer, K.W. Baldwin, and K.W. West, *Phys. Rev. Lett.* **90**, 056805 (2003).
31. V.M. Pudalov, M. Gershenson, and H. Kojima, *cond-mat/0110160*.
32. M. D'Iorio, V.M. Pudalov, and S.G. Semenchinsky, *Phys. Lett*. **A150**, 422 (1990); *Phys. Rev.* **B46**, 15992 (1992).
33. V.M. Pudalov, M. D'Iorio, and J.W. Campbell, *JETP Lett.* **57**, 608 (1993).
34. S.V. Kravchenko, A.A. Shashkin, D.A. Bloore, and T.M. Klapwijk, *Solid State Commun.* **116**, 495 (2000).
35. V.M. Pudalov, S.G. Semenchinskii, and V.S. Edel'man, *ZhETF* **89**, 1870 (1985) [*JETP* **62**, 1079 (1985)]; *Pis'ma Zh. Eksp. Teor. Fiz.* **41**, 325 (1985) [*JETP Lett.* **41**, 265 (1985)].
36. M. Hayne, A. Usher, J.J. Harris, and C.T. Foxon, *Phys. Rev.* **B46**, 9515 (1992).
37. A.P. Smith, A.H. Macdonald, and G. Gumbs, *Phys. Rev.* **B45**, 8829 (1992).
38. M. Fowler and R.E. Prange, *Physics Long Island City, N.Y.* **1**, 315 (1965).
39. S. Engelsberg and G. Simpson, *Phys. Rev.* **B2**, 1657 (1970).
40. G.W. Martin, D.L. Maslov, and M. Yu.Reizer, *Phys. Rev.* **B68**, 241309 R (2003).
41. Y. Adamov, I.V. Gornyi, and A.D. Mirlin, *Phys. Rev.* **B73**, 045426 (2006).
42. N.N. Klimov, D.A. Knyazev, O.E. Omel'yanovskii, V.M. Pudalov, H. Kojima, and M.E. Gershenson, *Phys. Rev.* **B78**, 195308 (2008).
43. G. Zala, B.N. Narozhny, and I.L. Aleiner, *Phys. Rev.* **B64**, 214204 (2001); *ibid*. **65**, 020201 (2001); *ibid.* **65**, 020201 (2002).
44. The quantum correction to the transport scattering rate $\tau_{\rm tr}^{-1}$ differs from that for the quantum scattering rate τ_D^{-1} by the factor $(1-\cos\phi)$ in the integrand, where ϕ is the scattering angle. According to the theory Ref. 43 the interaction corrections to the conductivity are determined by backscattering events for which $\phi \approx \pi$ and $(1-\cos\phi) \approx 2$.
45. A.A. Shashkin, S.V. Kravchenko, V.T. Dolgopolov, and T.M. Klapwijk, *Phys. Rev.* **B66**, 073303 (2002).
46. S.A. Vitkalov, K. James, B.N. Narozhny, M.P. Sarachik, and T.M. Klapwijk, *Phys. Rev.* **B67**, 113310 (2003).
47. V.M. Pudalov, M. Gershenson, and H. Kojima, *On the Electron–Electron Interactions in Two Dimensions*, in: *Fundamental Problems of Mesoscopic Physics*, I.V. Lerner et al. (eds.), Kluwer (2004), p. 309.
48. B.L. Al'tshuler, A.G. Aronov, and A. Yu.Zyuzin, *Pis'ma ZhETF* **35**, 15 (1962) [*JETP Lett.* **35**, 16 (1962)]; G.Y. Chitov and A.J. Millis, *Phys. Rev. Lett.* **86**, 5337 (2001); A.V. Chubukov and D.L. Maslov, *Phys. Rev.* **B60**, 121102 (2004).
49. A.M. Finkel'stein, *Z. Phys. B: Condens. Matter* **56**, 189 (1984); *Sov. Sci. Rev., Sect*. **A14**, 1 (1990); C. Castellani, C. Di Cast-

ro, and S. Sorella, *Phys. Rev.* **B34**, 1349 (1986); R. Raimondi, C. Castellani, and C. Di Castro, *Phys. Rev.* **B42**, 4724 (1990); C. Castellani, C. Di Castro, and P.A. Lee, *Phys. Rev.* **B57**, R9381 (1998); A. Punnoose and A.M. Finkel'stein, *Phys. Rev. Lett.* **88**, 16802 (2002).

50. V.M. Pudalov, M.E. Gershenson, H. Kojima, G. Brunthaler, A. Prinz, and G. Bauer, *Phys. Rev. Lett.* **91**, 126403 (2003).
51. U. Kunze and G. Lautz, *Surface Sci*. **142**, 314 (1984).
52. F.F. Fang, A.B. Fowler, and A. Hartstein, *Phys. Rev.* **B16**, 4446 (1977).
53. D.A. Knyazev, O.E. Omel'yanovskii, V.M. Pudalov, and I.S. Burmistrov, *JETP Lett.* **84**, 662 (2006).
54. S. Anissimova, S.V. Kravchenko, A. Punnoose, A.M. Finkel'stein, and T.M. Klapwijk, *Nature Phys*. **3**, 707 (2007).
55. D.A. Knyazev, O.E. Omel'yanovskii, V.M. Pudalov, and I.S. Burmistrov, *Phys. Rev. Lett.* **100**, 046405 (2008).